

Density Functional Studies on the Nazarov Reaction Involving Cyclic Systems

Andrea Cavalli,^{*[a]} Matteo Masetti,^[a] Maurizio Recanatini,^[a] Cristina Prandi,^[b] Antonio Guarna,^[c] and Ernesto G. Occhiato^{*[c]}

Abstract: Density functional theory (DFT) has been used to define the energy profiles of the Nazarov reaction involving cyclic systems. The calculations were carried out at the B3LYP/6-311G** level of theory and the solvent (dichloromethane) contribution was estimated by using the recently developed SM5.43R solvation model. DFT calculations were first carried out to determine the energy profiles associated with the electrocyclization reactions of 3-hydroxy- and 3-ethoxypentadienyl cations in which one of the double

bonds is embedded in O-heterocyclic and carbocyclic systems. In particular, the effects on the reaction rate of modifications to the substrate, as well as the presence of the heteroatom in the cycle, have been investigated. The torquoselectivity of the electrocyclization reaction was then explored with substi-

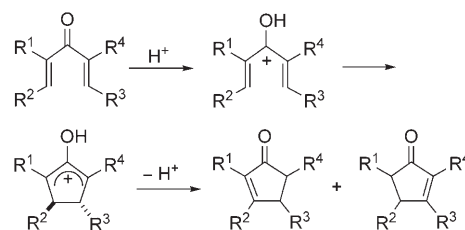
tuted O-heterocycles to understand the factors that control the stereochemical outcome of the process that preferentially provides 2,5-*trans*-disubstituted products. These DFT-based results rationally explain most of the experimental observations related to the Nazarov reaction of the substrates herein investigated and could be useful in the rational interpretation, and likely in the prediction, of the outcome of Nazarov reactions involving other cyclic systems.

Keywords: density functional calculations • electrocyclic reactions • Nazarov reaction • reaction mechanisms • torquoselectivity

Introduction

The acid-catalyzed cyclization reaction of a doubly α,β -unsaturated ketone, referred to as the Nazarov reaction, is currently one of the most versatile and powerful methods for the synthesis of five-membered carbocycles.^[1-7] Protonation of the ketone gives a cationic 4π -electron system, which un-

dergoes a conrotatory (under thermal conditions), electrocyclic process to form a five-membered ring (Scheme 1). The synthetic applications of the Nazarov reaction in its original



Scheme 1.

form have in the past been hampered by the harsh reaction conditions required (usually strong acids and high temperatures) and poor regioisomeric control. However, the abundance of five-membered carbocycles among natural products has inspired much research into the Nazarov reaction and these problems are nowadays solved by the use of Lewis acids as cyclization initiators,^[8-14] procedures called “directed Nazarov cyclization”^[15-19] and the “interrupted Nazarov reaction”,^[20-24] and the use of a variety of divinyl

[a] Dr. A. Cavalli, M. Masetti, Prof. M. Recanatini
Dipartimento di Scienze Farmaceutiche
Alma Mater Studiorum - Università di Bologna
Via Belmeloro 6, 40126 Bologna (Italy)
Fax: (+39)051-209-9735
E-mail: andrea.cavalli@unibo.it

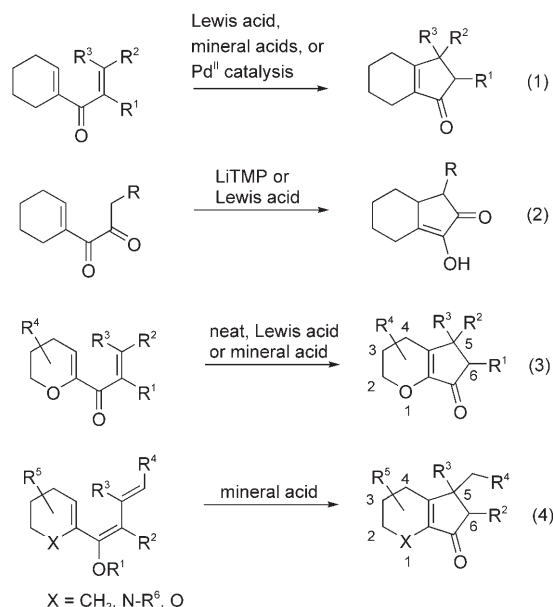
[b] Dr. C. Prandi
Dipartimento di Chimica Generale ed Organica Applicata
Università di Torino
Corso Massimo D’Azeglio, 48, 10125 Torino (Italy)

[c] Prof. A. Guarna, Dr. E. G. Occhiato
Dipartimento di Chimica Organica “U. Schiff”
Università di Firenze
Via della Lastruccia 13, 50019 Sesto Fiorentino (Italy)
Fax: (+39)055-457-3531
E-mail: ernesto.occhiato@unifi.it

Supporting information for this article is available on the WWW under <http://www.chemeurj.org/> or from the author.

ketone equivalents or pentadienyl cation precursors which undergo cyclization under milder conditions.^[3–7,25]

The potential of the Nazarov reaction in organic synthesis has grown enormously in the past few years as a consequence of a series of studies on the electrocyclization reactions of cyclic systems. Namely, systems in which one of the double bonds participating in the cyclization process is embedded in either a carbocycle or a heterocycle (O-heterocycle derivatives being predominant) [Eqs. (1)–(4)]. Both dienones [Eqs. (1) and (3)]^[9–11,13,14,26,27] and dienone equivalents [Eqs. (2) and (4)],^[25,28–30] which generate in situ an intermediate suitable to undergo electrocyclization, have very recently been used for this purpose. Moreover, strained polycyclic dienones have also been employed as substrates.^[31] In particular, O-heterocyclic derivatives [Eq. (3)] have successfully been employed in the first asymmetric variants of the Nazarov reaction carried out by chiral Lewis acid catalysis.^[13,14] Coordination of the metal center to the two oxygen atoms is thought to be crucial for the electrocyclization reaction^[10] as well as in amplifying the stereodifferentiation of the reaction.^[14]



Further advances in the Nazarov reaction involving cyclic systems have come from studies on the torquoselectivity^[3,32] of the process when alkyl substituents are present on the heterocyclic ring [Eqs. (3) and (4)].^[28,29] A surprisingly high remote stereocontrol was in fact observed in the formation of the new C5 stereocenter on the cyclopentenone moiety with 2-alkyl-substituted O-heterocycles [Eq. (3), R¹ = R³ = H, and Eq. (4), R² = R³ = H] as well as with the corresponding 2- and 4-alkyl-N-heterocyclic derivatives [Eq. (4), R² = R³ = H].^[28,29,33] Intriguingly, the exclusive formation of 2,5-*cis*-disubstituted N-heterocyclic derivatives was observed and plausibly imputed to steric interactions,^[28] whereas the reasons behind the prevailing formation of the 2,5-*trans*-dis-

substituted products in the hydrolysis of the corresponding dihydropyran derivatives was less clear.^[29]

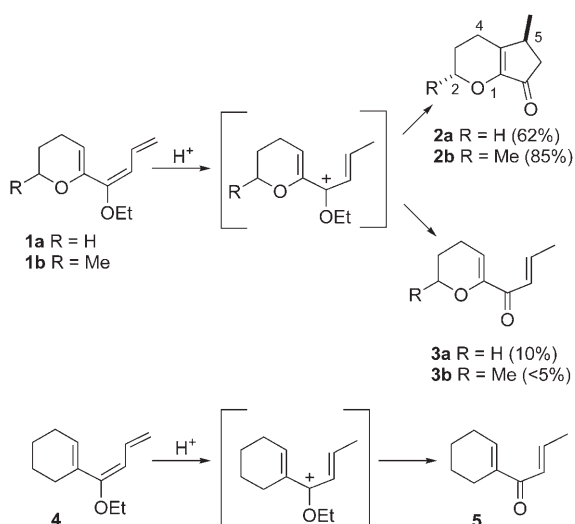
A survey of the literature concerning theoretical studies of the Nazarov reaction revealed some works aimed at the theoretical prediction of torquoselectivity in the electrocyclization process. However, these computational studies focused only on acyclic systems^[34–37] and on the retro-Nazarov reaction.^[38] In particular, the electronic^[34] and stereoelectronic^[35,36] effects exerted by β -substituents on simple pentadienyl cations were considered in the studies of Houk^[34] and Smith^[35,36] and their co-workers. The recent increased interest in the Nazarov reaction involving cyclic systems, as well as the substantial lack of ab initio and density functional theory (DFT) calculations on the torquoselectivity of the Nazarov reaction involving cyclic substrates for which further complications arise from the conformational mobility of the ring in which one double bond is embedded, prompted us to embark on a quantum chemical study of the key step of the Nazarov reaction, namely the electrocyclization, depicted in Equations (1), (3), and (4). In particular, a DFT-based study was carried out on the reaction in a vacuum and in dichloromethane as solvent using the continuum solvation model SM5.43R recently developed by Thompson et al.^[39] DFT calculations were first carried out to determine the energy profiles associated with the electrocyclization reactions of both O-heterocyclic and carbocyclic systems. Then, the torquoselectivity of the electrocyclization reaction of a 2-alkyl-substituted O-heterocycle was explored to understand the factors that affect the remote stereochemical control of the process that preferentially provides 2,5-*trans*-disubstituted products. In this paper, the results of these computations are presented and discussed in the light of previous quantum chemical calculations and experimental studies.

Results and Discussion

Energy profiles of the reaction mechanisms: The first issue we wanted to address was the reason behind the different reaction rates of the Nazarov reaction of divinyl ketones [Eqs. (1) and (3)] and the electrocyclization reaction carried out on the 6-(1-alkoxy-1,3-butadienyl)dihydropyrans shown in Equation (4) under mild acidic conditions.^[28,29] In this context, the role of the ring oxygen atom in the heterocycle was also evaluated.

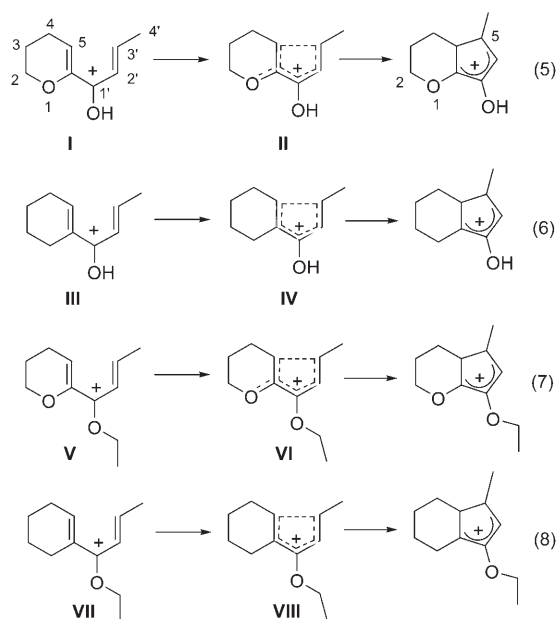
Referring to Scheme 2, 6-(1-ethoxy-1,3-butadienyl)dihydropyran derivatives **1** are thought to undergo protonation on the distal carbon atom of the ethoxydienyl moiety to produce a 3-ethoxypentadienylic cation with the requisite 4 π -electronic arrangement that undergoes the electrocyclization process. Cyclopenta[*b*]pyranones **2** are obtained in good yields when the reaction is carried out under mild acidic conditions (Amberlyst-15 resin in dichloromethane at room temperature).^[29]

The isolated divinyl ketones **3**, which are formed as minor products (less than 10%) in the hydrolysis of **1**, do not cy-



Scheme 2.

clize under the same conditions, but require stronger mineral acids to cyclopentannulate.^[40] Interestingly, the analogous carbocyclic derivative **4** (Scheme 2) simply hydrolyzes to the open-chain ketone **5** upon treatment with Amberlyst-15 and the latter cyclizes only upon treatment with stronger acids. To gain insights into the Nazarov reaction of these cyclic systems, we therefore considered the electrocyclization reactions of pentadienyl cations **I**, **III**, **V**, and **VII** [Eqs. (5)–(8)] as this is the rate-determining step of the whole cyclization process.^[3,7] Pentadienyl cations **I**, **III**, **V**, and **VII** are obtained by the protonation of substrates **3a**, **5**, **1a**, and **4** (Scheme 2), respectively. Cyclization then affords bicyclic oxyallyl intermediates [Eqs. (5)–(8)], which, after loss of a proton, give the final Nazarov products.



The energy profiles of the reaction coordinates of Equations (5)–(8) were calculated at the B3LYP/6-311G(d,p) level of theory, as were both the thermal correction and the solvent contribution (CH₂Cl₂; see the Computational Methods for details).

Figure 1 shows the DFT energy profiles and the structures of all the stationary points along the reaction coordinates, while in Table 1 the DFT-calculated electronic and free energies are reported. In particular, the energy profiles of the “conventional” Nazarov reaction [Eqs. (5) and (6)] are shown in Figure 1A and B, while the profiles of Equations (7) and (8), in which an alkyl group replaces the hydrogen atom on the oxygen of the pentadienyl cation, are reported in Figure 1C and D.

An important issue that had to be addressed in evaluating the reaction kinetics of the Nazarov reaction involving cyclic systems was the determination of the conformation of the six-membered ring in the lowest free-energy transition state (TS). Starting from a pentadienyl cation conformation as reported in Figure 2, a counterclockwise conrotation mode formally generates a boat-like TS. Conversely, a clockwise conrotation leads to a chair-like six-membered ring in the TS. However, the same TS conformation is also obtained starting from a pentadienyl cation in an inverted half-chair conformation by a counterclockwise conrotation (as done in the present work, see Figure 1).

In fact, the DFT calculations showed that the counterclockwise conrotation slightly distorts the initial half-chair conformation of the six-membered ring towards a twist-boat conformation in the TS. After bond formation, this conrotation mode eventually gave an oxyallyl cationic intermediate with the six-membered ring in a twist-boat conformation (see the profiles on the right side of Figure 1A–D). In the case of the clockwise conrotation (see the profiles on the left side of Figure 1A–D), the calculations showed that the formation of a chair-like TS (followed in the reaction profile by an oxyallyl intermediate with the six-membered ring in a chair-like conformation) is particularly evident with the carbocyclic systems (Figure 1 B and D, left).

In the case of the oxygenated derivatives (Figure 1A and C, left) the chair was reasonably distorted (flattened) by the conjugation of the oxygen atom with the π system as demonstrated by the C2-O1-C6-C5 dihedral angle value of -3.8° (in the case of the carbocyclic system, the corresponding C2-C1-C6-C5 torsion angle was 21.7° , see Table 2 for further details).

As for the energies of these transition states, it turned out that the activation free energy (ΔG^\ddagger) of the reaction that occurs through the distorted twist-boat TS was in all examined cases slightly lower than the ΔG^\ddagger associated with the clockwise conrotation mode (see Figure 1). In particular, the value of $\Delta\Delta G^\ddagger$ between the two conformations of the TS range from $1.3 \text{ kcal mol}^{-1}$ for the reaction of Equation (6) to $2.2 \text{ kcal mol}^{-1}$ for that of Equation (7). Angle and torsional strains, as well as stereoelectronic effects, could be the reasons for the generally higher stability of the distorted twist-boat transition states. Actually, differences in bond angles

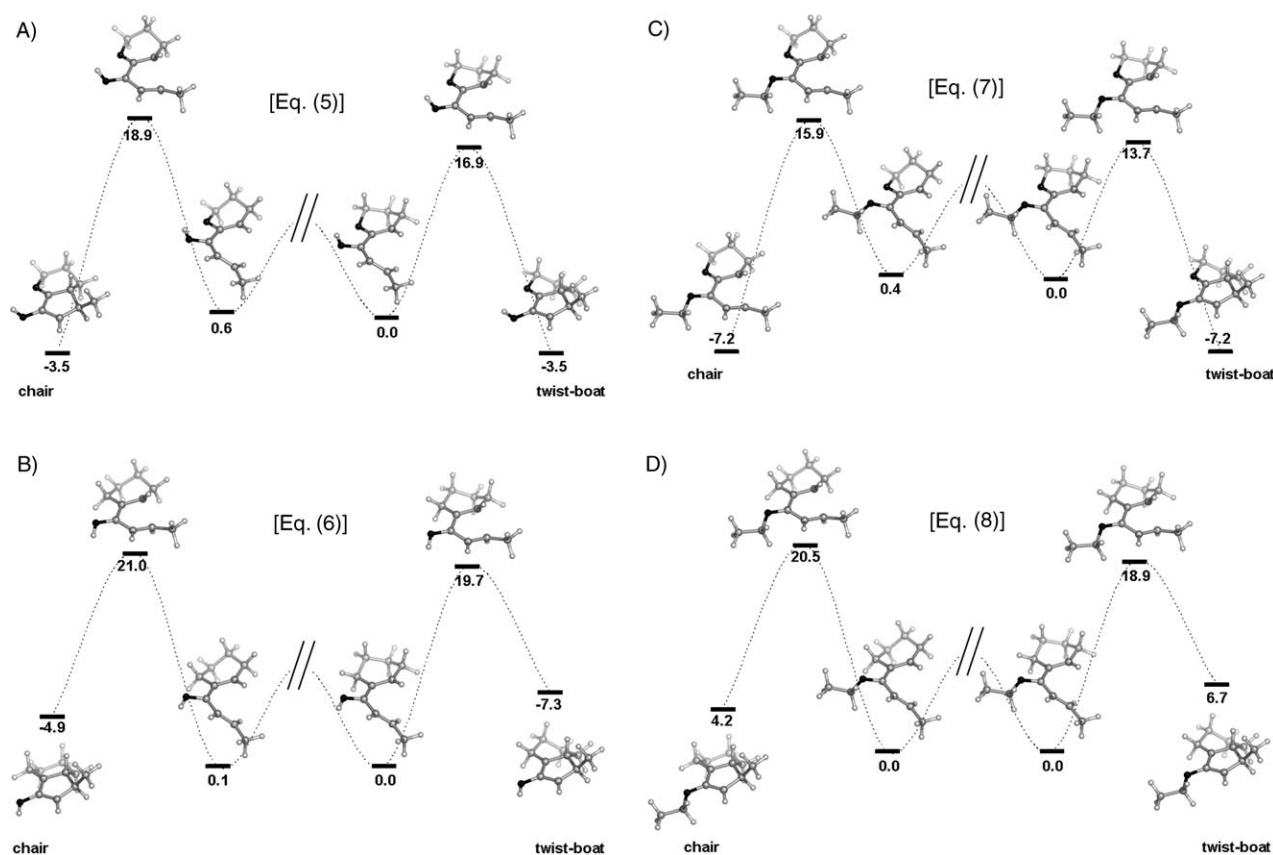


Figure 1. The free-energy profiles [kcal mol⁻¹] of A) Equation (5), B) Equation (6), C) Equation (7), and D) Equation (8). The free-energy profiles were drawn using the ΔG_{tot} values, computed as described in the Computational Methods.

Table 1. Relative electronic and free energies [kcal mol⁻¹] of the stationary points reported in Figure 1.^[a]

Equation		ΔE_{elec}	$\Delta(E_{\text{elec}} + \text{ZPVE})$	$\Delta G_{\text{gas-phase}}$	ΔG_{tot}
5 (Figure 1A)	react.	0.0	0.0	0.0	0.0
	TS _{twist-boat}	18.2 [‡]	17.6 [‡]	18.6 [‡]	16.9 [‡]
	prod.	-3.1	-1.9	-1.4	-3.5
5 (Figure 1A)	react.	0.6	0.5	0.4	0.6
	TS _{chair}	19.8 [‡]	19.4 [‡]	20.3 [‡]	18.9 [‡]
	prod.	-3.7	-2.5	-1.5	-3.5
6 (Figure 1B)	react.	0.0	0.0	0.0	0.0
	TS _{twist-boat}	19.6 [‡]	18.8 [‡]	19.8 [‡]	19.7 [‡]
	prod.	6.7	6.9	7.2	7.3
6 (Figure 1B)	react.	0.0	0.0	0.0	0.1
	TS _{chair}	20.6 [‡]	20.0 [‡]	20.9 [‡]	21.0 [‡]
	prod.	3.1	3.8	4.6	4.9
7 (Figure 1C)	react.	0.0	0.0	0.0	0.0
	TS _{twist-boat}	13.9 [‡]	13.7 [‡]	14.6 [‡]	13.7 [‡]
	prod.	-8.6	-6.8	-6.1	-7.2
7 (Figure 1C)	react.	0.5	0.5	0.4	0.4
	TS _{chair}	15.0 [‡]	15.4 [‡]	16.3 [‡]	15.9 [‡]
	prod.	-9.2	-7.5	-6.3	-7.2
8 (Figure 1D)	react.	0.0	0.1	0.0	0.0
	TS _{twist-boat}	19.8 [‡]	19.2 [‡]	20.1 [‡]	18.9 [‡]
	prod.	6.9	7.4	7.9	6.7
8 (Figure 1D)	react.	0.2	0.0	0.0	0.0
	TS _{chair}	20.8 [‡]	20.4 [‡]	21.3 [‡]	20.5 [‡]
	prod.	3.4	4.4	5.3	4.2

[a] ‡ indicates the activation free energies. ΔG_{tot} equals ΔG determined in the gas phase plus the solvent correction (see the Computational Methods). The part of Figure 1 the energy values refer to is reported in parentheses in the first column.

could be important in the case of pyran-containing transition states. In particular, taking into consideration Equation (5) as an example, in the chair-like TS the C2-O1-C6 bond angle was 120.0°, a value that differs greatly from the corresponding bond angle (114.6°) calculated for a DFT-optimized dihydropyran structure (the same C2-O1-C6 bond angle was 116.7° in the twist-boat TS). Also, in the chair-like TS the C2-O1-C6-C5 dihedral angle (-3.8°) was almost half that in the twist-boat structure (-6.6°), leading to greater eclipsing of the C2-O1 and C6-C5 bonds (in this case the shorter O1-C6 bond should emphasize this torsional strain). This was also true for the C3-C2-O1-C6 torsional angle, which was much smaller (-15.4°) than that in the twist-

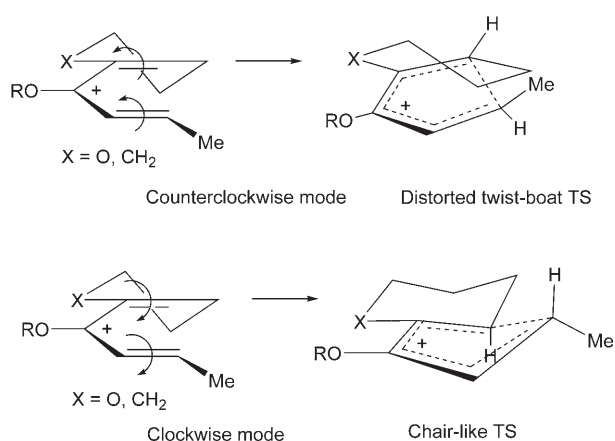


Figure 2. Transition states for the Nazarov reaction involving a cyclic system derived from a counterclockwise (above) and clockwise conrotation mode (below).

Table 2. Geometrical parameters of the stationary points reported in Figure 1.^[a]

Equation		C5–C3' [Å]	C2–X1–C6 [°]	C2–X1–C6–C5 [°]	C3–C2–X1–C6 [°]
5 (Figure 1A) X = O	react.	3.23	116.1	–12.8	44.8
	TS _{twist-boat}	2.18	116.7	–6.6	43.9
	prod.	1.55	115.6	3.5	46.8
5 (Figure 1A) X = O	react.	3.25	116.7	14.8	–42.9
	TS _{chair}	2.21	120.0	–3.8	–15.4
	prod.	1.55	120.6	10.8	–15.1
6 (Figure 1B) X = CH ₂	react.	3.14	112.4	–13.4	45.5
	TS _{twist-boat}	2.05	113.1	–0.2	39.1
	prod.	1.55	111.8	6.6	45.7
6 (Figure 1B) X = CH ₂	react.	3.17	111.5	21.0	–48.9
	TS _{chair}	2.08	113.1	21.7	–41.3
	prod.	1.55	109.2	40.1	–48.3
7 (Figure 1C) X = O	react.	3.13	116.0	–13.9	45.3
	TS _{twist-boat}	2.21	117.0	–8.8	44.7
	prod.	1.55	115.7	2.7	47.7
7 (Figure 1C) X = O	react.	3.16	116.3	12.6	–42.6
	TS _{chair}	2.23	120.3	–6.6	–14.4
	prod.	1.55	121.0	8.9	–14.0
8 (Figure 1D) X = CH ₂	react.	3.11	112.6	–12.9	45.0
	TS _{twist-boat}	2.04	113.3	0.0	38.8
	prod.	1.55	111.9	5.6	46.3
8 (Figure 1D) X = CH ₂	react.	3.14	111.7	20.5	–48.7
	TS _{chair}	2.07	113.1	22.0	–41.8
	prod.	1.54	109.5	47.5	–48.2

[a] The numbers refer to the reactant structure.

boat transition structure (43.9°). The same considerations were less easily applied to the carbocyclic systems [Eqs. (6) and (8)] in which no significant differences, in terms of angle and torsion strains, were identified. However, it was also possible that in all cases the differences in the activation free energies could be due to stereoelectronic reasons, in particular, to a slightly different superimposition of the orbitals of the atoms involved in the cyclization reaction, as previously suggested.^[29] As an example, the molecular orbital describing the newly forming bond in Equation (7) is shown in Figure 3. At the same isocontour level, such a molecular orbital seems to show a higher degree of completeness in the distorted twist-boat TS (Figure 3A) than in the

chair-like one (Figure 3B). Accordingly, as can be seen from the geometrical parameters of the stationary points (see Table 2), the distance between the cyclization termini in the twist-boat TS is in all cases slightly shorter than that in the chair-like TS.

Note here that the length of the newly forming bond in the Nazarov reaction of the carbocyclic systems [Eqs. (6) and (8)] ($d_{C5-C3'} = 2.05$ and 2.04 Å, respectively) was very similar to that previously predicted by calculations at the HF/6-31G* level of theory for an open-chain substrate ($d = 2.09$ Å).^[35] In contrast, the bond lengths in the O-heterocyclic systems were always longer (2.18–2.23 Å), suggesting that the TS of the Nazarov reaction involving O-heterocyclic systems might commonly be defined as an early TS, while the TS found for the carbocyclic compounds might be considered as a late TS. Accordingly, the reactions involving O-heterocyclic and carbocyclic systems are exothermic (Figure 1A and C) and endothermic (Figure 1B and D), respectively.

This is also in good agreement with the results of previous quantum mechanical calculations carried out to investigate the electrocyclic ring-closure of hydroxypentadienyl cations for which, generally, in the presence of an α -oxygen atom, the TS of the Nazarov reaction was found to be early.^[37]

Comparison of the kinetic profiles: In the light of the above considerations, in the following analysis we take into account only the electrocyclization reactions that occur through the distorted twist-boat TSs as these turned out to be energetically more favored than those involving a TS with a chair-like conformation. Looking at the energy profiles of Equations (5)–(8) reported in

Figure 1, it is clear that the reactions with the O-heterocyclic systems are both thermodynamically and kinetically more favored than the processes involving carbocyclic structures. Both the reactions involving the O-heterocyclic systems were in fact exothermic (see also Table 1), consistent with the early nature of their TSs, with the modified version of the Nazarov reaction in Equation (7) (Figure 1C) thermodynamically more favored than Equation (5) (Figure 1A) (the ΔG values being equal to -7.2 (Figure 1C) and -3.5 kcal mol⁻¹ (Figure 1A), respectively). Furthermore, by analyzing the energy profiles, it turns out that while the “classic” Nazarov reaction had a ΔG^\ddagger value of 16.9 kcal mol⁻¹ (Figure 1A), the ΔG^\ddagger value for the cyclization process

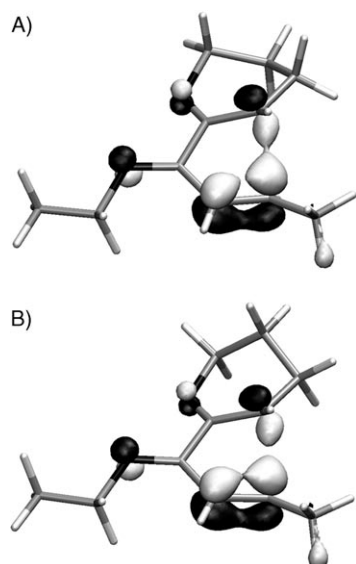


Figure 3. The molecular orbitals describing the newly forming bond plotted at the isocontour level of 0.095 a.u. for the reaction occurring through A) a distorted twist-boat TS and B) a chair-like TS.

reported in Equation (7) was equal to $13.7 \text{ kcal mol}^{-1}$ (Figure 1C). This latter result, in particular, is in striking agreement with experimental observations. Indeed, while compounds **1** (Scheme 2) cyclize to give the Nazarov products under mild acidic conditions at room temperature, compounds **3** do not under the same experimental conditions.^[29] Since the TSs of Equations (5) and (7) (i.e., **II** and **VI**) were found to be quite similar in terms of geometrical parameters (see Table 2 and the Supporting information) and in our opinion unable to explain a $\Delta\Delta G^\ddagger$ value of $3.2 \text{ kcal mol}^{-1}$, we reasoned that the origin of the different reaction rate was to be found in a greater stabilization of the protonated intermediate **I** [Eq. (5)] than of **V** [Eq. (7)]. After DFT-based optimization of **I** in dichloromethane, the conformation bearing an intramolecular hydrogen-bond interaction between the protonated carbonyl and the ring oxygen atom was found to be energetically far more stable ($\Delta\Delta G = 6.3 \text{ kcal mol}^{-1}$) than the one with the hydrogen atom pointing in the opposite direction. The lack of such a hydrogen-bond interaction in **V** could account for its higher energy relative to **I** and consequently for the lower activation free energy (ΔG^\ddagger) for Equation (7). The DFT-optimized geometries of two low-energy conformations of the intermediate with and without the above-mentioned hydrogen bond are shown in Figure 4A and B, respectively.

Our finding that a hydrogen atom is shared by the two oxygen atoms in a structure such as **I** is consistent with the observation that transition metals are presumably bound in a bidentate fashion to very similar substrates in efficient Lewis acid catalyzed Nazarov reactions, while such an efficient catalysis has been reported not to occur with the corresponding carbocyclic systems.^[10,13,14] On the basis of these results, we can conclude that the main difference between the rates of the “classic” Nazarov reaction [Eq. (5)] and the

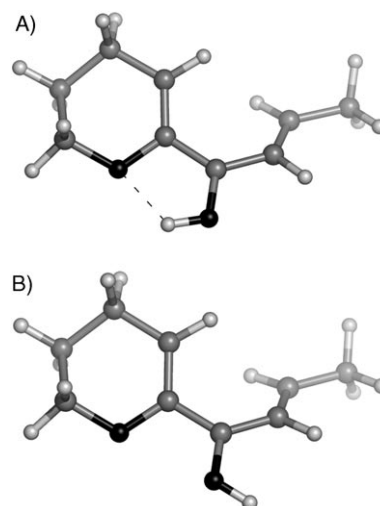


Figure 4. Low-energy conformations of the protonated intermediate **I**. A) The global minimum conformer (optimized at the DFT level in CH_2Cl_2) possesses a greatly stabilizing intramolecular hydrogen-bond, whereas if the hydrogen-bond interaction was not established as in B), the conformation turned out to be less stable by as much as $6.3 \text{ kcal mol}^{-1}$.

“modified” version [Eq. (7)] is due to a greater stabilization of the starting charged intermediate and to a lesser extent to the different geometrical and electronic parameters of the reaction’s transition states.

The effect of the heterocyclic oxygen atom: As we have already mentioned, the electrocyclization reaction of carbocyclic systems such as **4** (Scheme 2) does not take place under the same mild acidic conditions under which the electrocyclization reaction of the oxygenated derivatives **1** occurs.^[29] This somehow has to be related to the presence of the α -oxygen atom within the six-membered ring. In the light of the experimental observations, we focused on the effect of the heterocyclic oxygen atom on the reaction rate by comparing the kinetics of Equations (5)–(8). Again, here, we discuss only the reactions that occur through the distorted twist-boat TS as these were energetically most favored. In agreement with the experimental observations, it turned out that the values of ΔG^\ddagger for Equations (6) and (8) (i.e., for the reactants lacking the oxygen heterocyclic atom) were too high to allow the reaction to occur under mild conditions. In fact, the DFT-computed ΔG^\ddagger values were 19.7 and $18.9 \text{ kcal mol}^{-1}$ for the “classic” Nazarov (Figure 1B) and the “modified” Nazarov reactions (Figure 1D), respectively. Interestingly enough, for the Nazarov reaction of Equation (6), the increase in free energy of the protonated intermediate **III**, due to the lack of the intramolecular hydrogen-bond that is present in the O-heterocyclic system [**I** of Equation (5), see also Figure 3A], was counterbalanced by the lack of the stabilizing effect on the positive charge of the TS exerted by the heterocyclic oxygen atom.^[37] This stabilizing effect has been previously invoked by us^[28,29] to explain why the reaction of Equation (7) could occur under mild acidic conditions ($\Delta G^\ddagger = 13.7 \text{ kcal mol}^{-1}$) at room temperature,

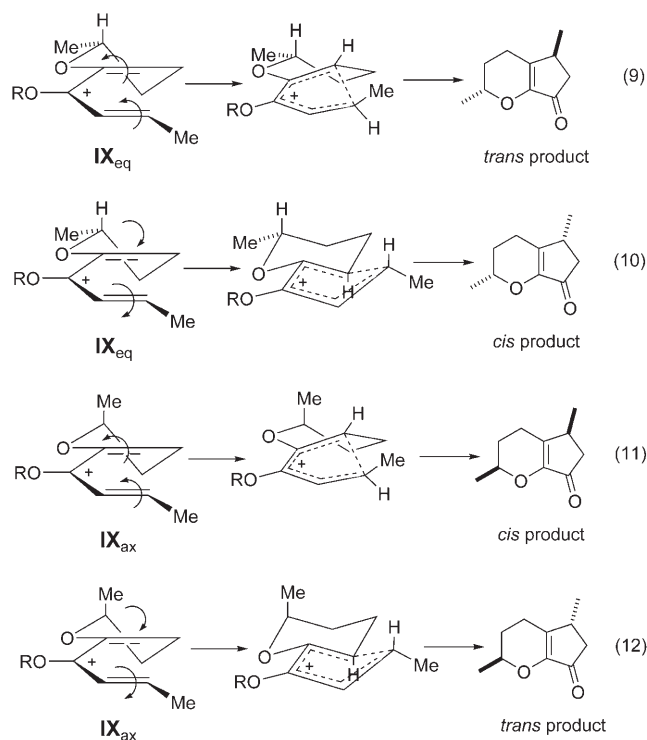
while the reaction of Equation (8) ($\Delta G^\ddagger = 18.9 \text{ kcal mol}^{-1}$) requires more drastic conditions. Here, to demonstrate such an effect, we calculated the atomic partial charges on the oxygen atom of the positively charged intermediate **V** and the TS **VI** of Equation (7) by the RESP-fitting procedure (see the Computational Methods). It turned out that the heterocyclic oxygen atom had a partial atomic charge of -0.32 in **V**, but of only -0.26 in **VI**. The significant decrease in the partial negative charge on the oxygen atom found in **VI** demonstrates that the heteroatom effectively conjugates with the p orbitals of the TS, thus providing a greater stabilization effect on the positive charge of the TS relative to that of the starting intermediate, in good agreement with the results previously reported by de Lera and co-workers on smaller molecular systems.^[37] Furthermore, we also carried out single-point calculations in which the positive charge on the system was neutralized by the addition of one electron to both the starting intermediate **V** and the TS **VI** (see the Computational Methods). It turned out that the electronic energy barrier to the electrocyclization reaction was $\sim 36 \text{ kcal mol}^{-1}$ (vs. $13.9 \text{ kcal mol}^{-1}$, see Table 1), this increase being mainly due to a much greater stabilization of the starting intermediate **V** ($\Delta \text{electronic energy} = -118.4 \text{ kcal mol}^{-1}$) with respect to the TS **VI** ($\Delta \text{electronic energy} = -96.0 \text{ kcal mol}^{-1}$).

The torquoselectivity: The last issue investigated in this study concerned the effect of a 2-alkyl substituent on the six-membered cycle on the torquoselectivity of the electrocyclization reaction. This is a very intriguing and synthetically important^[33] aspect of the Nazarov reaction involving cyclic systems: in the case of pyran derivative **1b**, (Scheme 2), but also in dienones such as **3b** bearing a 2-methyl group on the heterocycle, the electrocyclization reaction leads to the preferential formation of the *trans*-2,5-disubstituted compound **2b** (Scheme 2) (*trans/cis* ratio = 16:1).^[29] The product distribution in the electrocyclization reaction of pyran derivative **1b** might be the result of a complex combination of thermodynamic (conformer populations) and kinetic factors (activation free energies).

The reaction intermediate **IX** can exist in two equilibrating conformations [Eqs. (9)–(12)] in which the 2-methyl group is axially or equatorially oriented (**IX_{eq}** and **IX_{ax}**). The computation of the free-energy difference between the two conformers **IX_{eq}** and **IX_{ax}** revealed the equatorial conformation to be more stable than the axial one by $1.9 \text{ kcal mol}^{-1}$, which corresponds to a population ratio of 20:1 for the two conformers. The equatorial conformer **IX_{eq}** gives the *trans* product through a distorted twist-boat TS [Eq. (9)], that is, through a counterclockwise conrotation, and the *cis* product through a clockwise conrotation [Eq. (10)] through a chair-like TS. The reverse applies to the axial conformer **IX_{ax}** [Eqs. (11) and (12)]. Again, in these cases, the TSs deriving from a clockwise conrotation were obtained by inverting the half-chair in the starting pentadienyl cations and imposing a counterclockwise conrotation. The DFT energy profiles and the structures of all the stationary points along the reaction

coordinates of Equations (9)–(12) are shown in Figure 5 and the DFT-calculated electronic and free energies are reported in Table 3. From these calculations, it clearly emerges that the electrocyclization reaction of the equatorial conformer through a distorted twist-boat TS is the kinetically preferred process [$\Delta G^\ddagger = 13.8 \text{ kcal mol}^{-1}$, Eq. (9), and Figure 5A], as in the case of the unsubstituted substrates previously treated, whereas all the other pathways [Eqs. (10)–(12) and Figure 5B–D] exhibited higher barriers in the narrow range of 14.8 – $15.3 \text{ kcal mol}^{-1}$. Interestingly, with the axially oriented methyl group the clockwise conrotation, which gives the *trans* product, was slightly favored above the counterclockwise one, which provides the *cis* product. Taking into account the calculated population ratio of 20:1 for the two conformers, the counterclockwise cyclization of the equatorial conformer **IX_{eq}** is the one that principally contributed to the formation of the product possessing a relative 2,5-*trans* stereochemistry, which actually is the major diastereomer experimentally found in the final reaction mixture. The observed 16:1 product ratio for the *trans* and *cis* isomers eventually results from the minor contribution of the less favored pathways of Equations (10) and (11) by which the two differently populated conformers reacted. We are confident that the present description could be useful in driving future experiments aimed at preferentially obtaining one diastereomer by the Nazarov reaction of cyclic systems.

As a last observation, with the axial methyl group the two competitive pathways of Equations (11) and (12) are kinetically almost equally favored. At least with these oxygenated systems, therefore, it seems that there are no particularly unfavorable interactions between the axial group and the C5–C3' forming bond in the TS that could prevent a clockwise



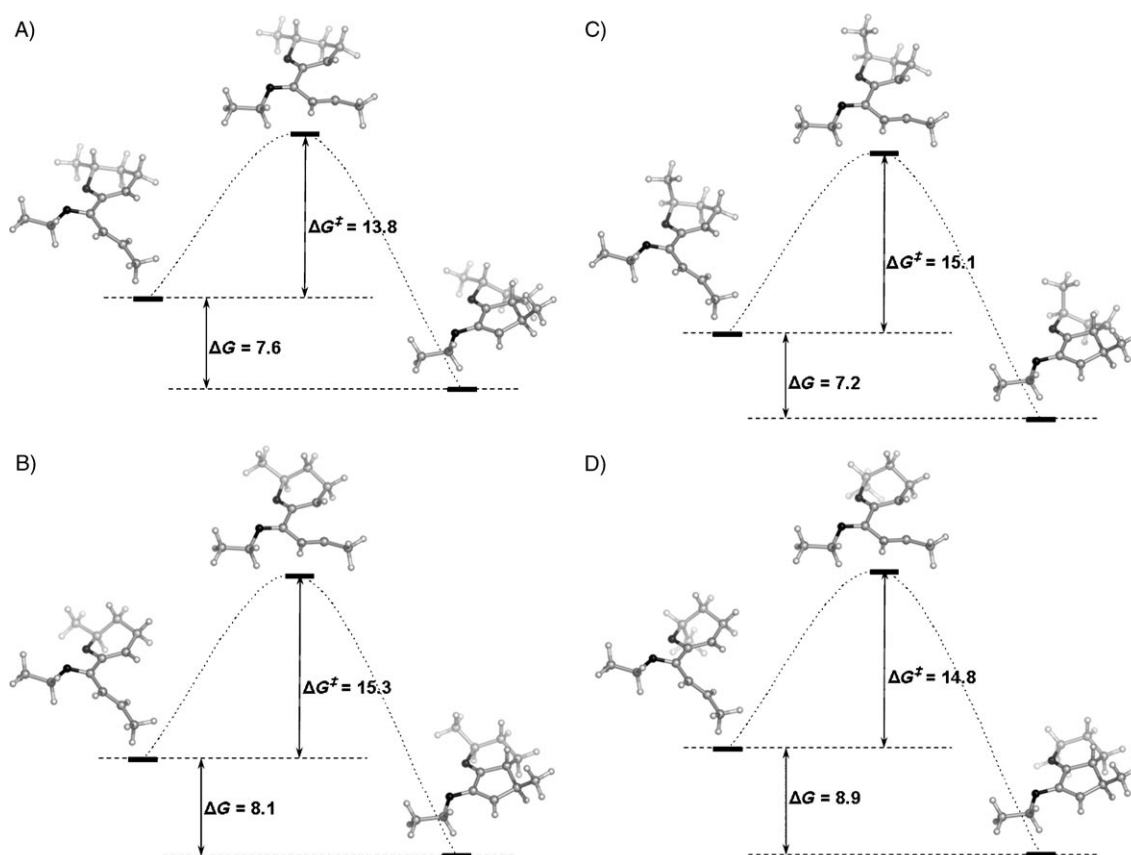


Figure 5. The free-energy profiles [kcal mol^{-1}] of A) Equation (9), B) Equation (10), C) Equation (11), and D) Equation (12). The free-energy profiles were drawn using the ΔG_{tot} values, computed as described in the Computational Methods.

Table 3. Relative electronic and free energies [kcal mol^{-1}] of the stationary points reported in Figure 5.^[a]

Equation		ΔE_{elec}	$\Delta(E_{\text{elec}} + \text{ZPVE})$	$\Delta G_{\text{gas-phase}}$	ΔG_{tot}
9 (Figure 5A)	react.	0.0	0.0	0.0	0.0
	TS _{twist-boat}	13.5 [†]	13.2 [†]	14.2 [†]	13.8 [†]
	prod.	-9.6	-8.6	-6.9	-7.6
10 (Figure 5B)	react.	0.0	0.0	0.0	0.0
	TS _{chair}	14.8 [†]	14.6 [†]	15.5 [†]	15.3 [†]
	prod.	-10.8	-9.0	-7.9	-8.1
11 (Figure 5C)	react.	0.0	0.0	0.0	0.0
	TS _{twist-boat}	13.5 [†]	15.2 [†]	15.6 [†]	15.1 [†]
	prod.	-9.2	-7.6	-6.8	-7.2
12 (Figure 5D)	react.	0.0	0.0	0.0	0.0
	TS _{chair}	14.2 [†]	14.0 [†]	14.9 [†]	14.8 [†]
	prod.	-11.2	-9.6	-8.6	-8.9

[a] [†] indicates the activation free energies. ΔG_{tot} equals ΔG determined in the gas phase plus the solvent correction (see the Computational Methods). The part of Figure 5 the energy values refer to is reported in parentheses in the first column.

conrotation, as has been suggested for the analogous N-heterocyclic systems (which exclusively give the *cis* product).^[28]

Conclusion

In this paper, we report the first DFT-based study of the Nazarov reaction involving cyclic systems. We have investigated the reaction coordinates of the “classic” Nazarov electrocyclicization reaction of divinyl ketones starting from the

appropriate cationic intermediates. The reactions of both O-heterocyclic and carbocyclic derivatives have been studied. It turned out that in all cases the value of ΔG^{\ddagger} is sufficiently high to prevent the reaction occurring under mild acidic conditions at room temperature, as experimentally observed. In the case of the O-heterocyclic derivatives, in particular, the high ΔG^{\ddagger} value is caused by the stabilization of the pentadienyl cation intermediate by an intramolecular

hydrogen-bond which compensates for the stabilization of the positive charge in the TS by the heterocyclic α -oxygen atom. The Nazarov reaction of the closely related 3-ethoxy-pentadienylic cations, experimentally obtained by protonation of the distal double bond of 6-(1-ethoxy-1,3-butadienyl)dihydropyran and the corresponding carbocyclic derivatives, has also been computationally studied. By inspection of the reaction coordinates, it is clear that the only process that these substrates could undergo at room temperature under mild acidic conditions was that involving the O-heter-

ocyclic system ($\Delta G^\ddagger = 13.7 \text{ kcal mol}^{-1}$), whose lower activation barrier (relative to other profiles) was mainly due to the stabilization of the positive charge in the TS through conjugation with the heterocyclic oxygen atom. This reaction was also shown to be strongly exothermic ($\Delta G = -7.2 \text{ kcal mol}^{-1}$), further confirming the experimental observations. As a general rule, a conrotation mode leading to the formation of a TS with a six-membered ring in a twist-boat-like conformation was preferred owing to better orbital overlap at the level of the newly forming C5–C3' bond.

As for the torquoselectivity of the electrocyclization process that these systems experience when an alkyl substituent is present in the 2-position, the experimental observation is that the *trans/cis* ratio in the reaction products is 16:1. We were able to explain this ratio through the observation that the equatorial conformer is the most populated (20:1) and that it preferentially provides the 2,5-*trans*-disubstituted product through a process involving a twist-boat-like TS. The experimentally observed 16:1 product ratio of *trans* and *cis* products is an eventual result of the minor contributions of less favored competitive pathways by which the two differently populated conformers react.

The present DFT-based results were able to rationally explain most of the experimental observations related to the Nazarov reaction of the examined substrates and should prove helpful in the interpretation, and possibly in the prediction, of the results of Nazarov reactions involving other cyclic systems. Studies on Nazarov reactions involving N-heterocyclic compounds are currently underway.

Computational Methods

The gas-phase quantum-chemical calculations were performed using the Gaussian 03 (G03)^[41] suite of programs. For all stationary points, both geometry and analytical frequency calculations were carried out at the DFT level of theory by using the restricted B3LYP hybrid functional^[42] which has already been successfully employed in the description of analogous pericyclic reactions.^[37,43] Pople's 6-311G(d,p) basis set, which provides a single set of polarization functions for both the heavy and the hydrogen atoms, was employed. Geometry optimizations were carried out in the gas-phase using the G03 default convergence criteria with the Berny algorithm^[44] and the synchronous transit-guided quasi-Newton (STQN) method^[45] (QST2 routine implemented in G03) for the local minima and saddle points, respectively. Frequency calculations at the reference temperature of 298.15 K were performed both to characterize stationary points and to calculate their thermodynamic properties. Since this study focused on the free-energy differences (relative free-energy values) between reactants and products and between reactants and saddle points, no scaling factors were applied to the computed zero-point vibrational energies. For all the reaction transition states reported hereafter, the diagonalized mass-weighted Hessian matrix exhibited only one negative eigenvalue, revealing a first-order saddle point. Moreover, for each identified saddle point, the corresponding normal mode (related to the negative eigenvalue) involved nuclear displacements along the investigated reaction coordinate. In addition, as further evidence for the proper reaction path, some intrinsic reaction calculations (IRC)^[46,47] were also carried out on selected systems at the B3LYP/6-311G(d,p) level of theory (data not shown). Finally, the solvent contribution for all stationary points was assessed by means of the SMxGAUSS 2.0.1 program.^[39] SMxGAUSS is a new quantum mechanics package that performs liquid-phase calculations by using the SMx suite of universal solvation models

developed by Truhlar and co-workers.^[48] The latter is a set of continuum solvation models based on the generalized Born approximation in which first-solvation effects are modeled with atomic surface tension functionals that are proportional to the solvent-accessible surface area (SASAs) of the atoms in the solute.^[48] These functionals are parametrized to properly reproduce a wide set of free energies of solvation in water and in organic solvents. Notably, the SM5.43R universal model predicts both the aqueous and organic free energies of solvation^[48] more accurately than the polarizable continuum model (PCM) methods.^[49] Here, single-point self-consistent reaction-field (SCRf) calculations on the previously converged geometries were carried out in an implicit dichloromethane (CH_2Cl_2) continuum by using the SM5.43R solvation model. The mPW1K hybrid functional was chosen to describe the solute, as it has been suggested for calculating kinetics,^[48] along with the 6-31G(d) basis set. Owing to the differences in the level of theory used for the gas-phase calculations and the evaluation of the solvent contributions, the solvent correction to the free-energy differences must definitely be intended as an independent additive term. In short the relative molar free energies were calculated using Equation (13).

$$\Delta G_{\text{tot}} = (\Delta G_{\text{gas-phase}})^{\text{B3LYP/6-311G**}} + (\Delta G_{\text{solvation}})^{\text{mPW1K/6-31G*}} \quad (13)$$

The gas-phase free energy is defined by Equation (14), where ΔE_{elec} , ΔZPE , $\Delta H_{\text{vibr-rot}}(T)$, and $\Delta S(T)$ are the electronic energy, the zero-point energy, the vibrational-rotational enthalpy, and the total entropy calculated at 298.15 K, respectively.

$$\Delta G_{\text{gas-phase}} = \Delta E_{\text{elec}} + \Delta \text{ZPE} + \Delta H_{\text{vibr-rot}}(T) - T\Delta S(T) \quad (14)$$

The solvation free energy was calculated with Equation (15),^[48] where ΔE_{elec} and $\Delta G_{\text{vir-rot}}$ are the changes in electronic energy and vibrational-rotational free energy, respectively, following solvation. G_p is the electronic polarization energy, and G_{CDS} is a semiempirical term (see the report by Thompson et al. for details^[39]).

$$\Delta G_{\text{solvation}} = \Delta E_{\text{elec}} + G_p + G_{\text{CDS}} + \Delta G_{\text{vibr-rot}} \quad (15)$$

Some calculations were carried out by adding one electron to the systems in order to estimate the effects of positive charge on both the reactants and the transition states (see Results and Discussion). These calculations were carried out by using the restricted open-shell ROB3LYP functional (employing the same basis set as reported above) as the spin multiplicity passed from 1 to 2.

The partial charges were computed following the standard two-stage RESP fitting procedure,^[50,51] fitting first the polar areas by using weak hyperbolic restraints (0.0005 a.u.) and then by fitting the remaining areas by imposing equivalencies and by imposing a stronger restraint (0.001 a.u.). The quantum electrostatic potential used was sampled by adapting the Merz–Kollman–Singh (MKS) scheme,^[52,53] namely by using 10 concentric layers at the default level of spacing, a surface density of 6 points \AA^{-2} , and the default MKS van der Waals radii (as suggested elsewhere^[54]).

For the intermediates of Equations (9)–(12) (see below), one of the two enantiomers was arbitrarily chosen for the study.

All calculations were performed on a Linux cluster by employing an open Mosix architecture.

Acknowledgements

We thank Mr. Alessandro Pacetti for his technical assistance and Dr. Marco Garavelli for useful discussions. MIUR-COFIN is gratefully acknowledged for financial support.

[1] I. N. Nazarov, I. B. Torgov, L. N. Terekhova, *Izv. Akad. Nauk. SSSR old Khim. Nauk.* **1942**, 200.

- [2] E. A. Braude, W. F. Forbes, *J. Chem. Soc.* **1953**, 2208–2216.
- [3] K. L. Habermas, S. E. Denmark, T. D. Jones, *Org. React.* **1994**, *45*, 1–158.
- [4] S. E. Denmark in *Comprehensive Organic Synthesis, Vol. 5* (Eds.: B. M. Trost, I. Fleming), Pergamon Press, Oxford, **1991**, pp. 751–784.
- [5] M. A. Tius, *Eur. J. Org. Chem.* **2005**, 2193–2206.
- [6] H. Pellissier, *Tetrahedron* **2005**, *61*, 6479–6517.
- [7] A. J. Frontier, C. Collison, *Tetrahedron* **2005**, *61*, 7577–7606.
- [8] L. A. Paquette, W. E. Fristad, D. S. Dime, T. R. Bailey, *J. Org. Chem.* **1980**, *45*, 3017–3028.
- [9] W. He, X. Sun, A. J. Frontier, *J. Am. Chem. Soc.* **2003**, *125*, 14278–14279.
- [10] M. Janka, W. He, A. J. Frontier, R. Eisenberg, *J. Am. Chem. Soc.* **2004**, *126*, 6864–6865.
- [11] P. Chiu, S. Li, *Org. Lett.* **2004**, *6*, 613–616.
- [12] V. K. Aggarwal, A. J. Belfield, *Org. Lett.* **2003**, *5*, 5075–5078.
- [13] G. Liang, S. N. Gradl, D. Trauner, *Org. Lett.* **2003**, *5*, 4931–4934.
- [14] G. Liang, D. Trauner, *J. Am. Chem. Soc.* **2004**, *126*, 9544–9545.
- [15] S. E. Denmark, T. K. Jones, *J. Am. Chem. Soc.* **1982**, *104*, 2642–2645.
- [16] T. K. Jones, S. E. Denmark, *Helv. Chim. Acta* **1983**, *66*, 2377–2396.
- [17] M. R. Peel, C. R. Johnson, *Tetrahedron Lett.* **1986**, *27*, 5947–5950.
- [18] J. Ichikawa, J. Miyazaki, M. Fujiwara, T. Minami, *J. Org. Chem.* **1995**, *60*, 2320–2321.
- [19] J. Ichikawa, M. Fujiwara, T. Okauchi, T. Minami, *Synlett* **1998**, 927–929.
- [20] S. Giese, F. G. West, *Tetrahedron* **2000**, *56*, 10221–10228.
- [21] Y. Wang, A. M. Arif, F. G. West, *J. Am. Chem. Soc.* **1999**, *121*, 876–877.
- [22] J. A. Bender, A. E. Blize, C. C. Browder, S. Giese, F. G. West, *J. Org. Chem.* **1998**, *63*, 2430–2431.
- [23] J. A. Bender, A. M. Arif, F. G. West, *J. Am. Chem. Soc.* **1999**, *121*, 7443–7444.
- [24] A. Yungai, F. G. West, *Tetrahedron Lett.* **2004**, *45*, 5445–5448.
- [25] W. A. Batson, D. Sethumadhavan, M. A. Tius, *Org. Lett.* **2005**, *7*, 2771–2774.
- [26] C. Bee, E. Leclerc, M. A. Tius, *Org. Lett.* **2003**, *5*, 4927–4930.
- [27] F. Douelle, L. Tal, F. Greaney, *Chem. Commun.* **2005**, 660–662.
- [28] E. G. Occhiato, C. Prandi, A. Ferrali, A. Guarna, P. Venturello, *J. Org. Chem.* **2003**, *68*, 9728–9741.
- [29] C. Prandi, A. Ferrali, A. Guarna, P. Venturello, E. G. Occhiato, *J. Org. Chem.* **2004**, *69*, 7705–7709.
- [30] C. Prandi, A. Deagostino, P. Venturello, E. G. Occhiato, *Org. Lett.* **2005**, *7*, 4345–4348.
- [31] R. D. Mazzola, T. D. White, H. Vollmer-Snarr, F. G. West, *Org. Lett.* **2005**, *7*, 2799–2801.
- [32] K. N. Houk in *Strain and its implications in organic chemistry* (Eds.: A. de Meijere, S. Blechert), Kluwer Academic Publisher, Dodrecht, **1989**, pp. 25–37.
- [33] E. G. Occhiato, C. Prandi, A. Ferrali, A. Guarna, *J. Org. Chem.* **2005**, *70*, 4542–4545.
- [34] E. A. Kallel, K. N. Houk, *J. Org. Chem.* **1989**, *54*, 6006–6008.
- [35] D. A. Smith, C. W. Ulmer, II, *Tetrahedron Lett.* **1991**, *32*, 725–728.
- [36] D. A. Smith, C. W. Ulmer, II, *J. Org. Chem.* **1997**, *62*, 5110–5115.
- [37] O. N. Faza, C. S. López, R. Álvarez, Á. R. de Lera, *Chem. Eur. J.* **2004**, *10*, 4324–4333.
- [38] M. Harmata, P. R. Schreiner, D. R. Lee, P. L. Kirchhoefer, *J. Am. Chem. Soc.* **2004**, *126*, 10954–10957.
- [39] J. D. Thompson, C. J. Cramer, D. G. Truhlar, *J. Phys. Chem. A* **2004**, *108*, 6532–6542.
- [40] Compounds **3** and **5** cyclize to give the Nazarov products in neat TFA or by treatment with a 0.2 M solution of CF₃SO₃H.
- [41] Gaussian 03, M. J. Frisch, G. W. Trucks, H. B. Schlegel, G. E. Scuse-ria, M. A. Robb, J. R. Cheeseman, V. G. Zakrzewski, J. A. Montgo-mery, Jr., R. E. Stratmann, J. C. Burant, S. Dapprich, J. M. Millam, A. D. Daniels, K. N. Kudin, M. C. Strain, O. Farkas, J. Tomasi, V. Barone, M. Cossi, R. Cammi, B. Mennucci, C. Pomelli, C. Adamo, S. Clifford, J. Ochterski, G. A. Petersson, P. Y. Ayala, Q. Cui, K. Mo-rokuma, D. K. Malick, A. D. Rabuck, K. Raghavachari, J. B. Fores-man, J. Cioslowski, J. V. Ortiz, B. B. Stefanov, G. Liu, A. Liashenko, P. Piskorz, I. Komaromi, R. Gomperts, R. L. Martin, D. J. Fox, T. Keith, M. A. Al-Laham, C. Y. Peng, A. Nanayakkara, C. Gonzalez, M. Challacombe, P. M. W. Gill, B. G. Johnson, W. Chen, M. W. Wong, J. L. Andres, M. Head-Gordon, E. S. P. Replogle, J. A. Pople, Gaussian, Inc., Pittsburgh, PA, **2003**.
- [42] A. D. Becke, *J. Chem. Phys.* **1993**, *98*, 1372–1377.
- [43] B. Iglesias, Á. R. de Lera, J. Rodríguez-Otero, S. López, *Chem. Eur. J.* **2000**, *6*, 4021–4033.
- [44] C. Peng, P. Y. Ayala, H. B. Schlegel, M. J. Frisch, *J. Comput. Chem.* **1996**, *17*, 49–56.
- [45] C. Peng, H. B. Schlegel, *Isr. J. Chem.* **1993**, *33*, 449–454.
- [46] C. Gonzalez, H. B. Schlegel, *J. Chem. Phys.* **1989**, *90*, 2154–2162.
- [47] C. Gonzalez, H. B. Schlegel, *J. Phys. Chem.* **1990**, *94*, 5523–5527.
- [48] J. D. Thompson, C. J. Cramer, D. G. Truhlar, *Theor. Chem. Acc.* **2005**, *113*, 107–131.
- [49] S. Miertus, E. Scrocco, J. Tomasi, *Chem. Phys.* **1981**, *55*, 117–129.
- [50] C. I. Bayly, P. Cieplak, W. D. Cornell, P. A. Kollman, *J. Phys. Chem.* **1993**, *97*, 10269–10280.
- [51] W. D. Cornell, P. Cieplak, C. I. Bayly, P. A. Kollman, *J. Am. Chem. Soc.* **1993**, *115*, 9620–9631.
- [52] U. C. Singh, P. A. Kollman, *J. Comput. Chem.* **1983**, *4*, 129–145.
- [53] B. H. Besler, K. M. Merz, P. A. Kollman, *J. Comput. Chem.* **1990**, *11*, 431–439.
- [54] E. Sigfridsson, U. Ryde, *J. Comput. Chem.* **1998**, *19*, 377–395.

Received: November 8, 2005
Published online: January 23, 2006